ЖЭТФ, 2010, том 138, вып. 4 (10), стр. 709–716

NUCLEAR ^{111}Cd PROBES DETECT A HIDDEN SYMMETRY CHANGE UNDER THE $\gamma \to \alpha$ TRANSITION IN CERIUM CONSIDERED ISOSTRUCTURAL FOR 60 YEARS

A. V. Tsvyashchenko [a,b*], ***A. V. Nikolaev*** [b,e**], ***A. I. Velichkov*** [c], ***A. V. Salamatin*** [c], ***L. N. Fomicheva*** [a], ***G. K. Ryasny*** [b], ***A. A. Sorokin*** [b], ***O. I. Kochetov*** [c], ***M. Budzynski*** [d]

[a] *Vereshchagin Institute for High Pressure Physics, Russian Academy of Sciences 142190, Troitsk, Moscow Region, Russia*

[b] *Skobeltsyn Institute of Nuclear Physics, Lomonosov Moscow State University 119991, Moscow, Russia*

[c] *Joint Institute for Nuclear Research 141980, Dubna, Moscow Region, Russia*

[d] *Institute of Physics, Curie-Sklodowska University 20-031, Lublin, Poland*

[e] *Institute of Physical Chemistry and Electrochemistry, Russian Academy of Sciences 119991, Moscow, Russia*

Received March 5, 2010

We use the time-differential perturbed angular correlation technique to study nuclear electric quadupole hyperfine interactions of probe ^{111}Cd nuclei in cerium lattice sites at room temperature under pressures up to 8 GPa. We have found that the well known $\gamma \to \alpha$ phase transition in cerium is not isostructural. In α-Ce, the probe ^{111}Cd nuclei reveal a quadrupole electron charge density component that is absent in γ-Ce. The hidden spacial structure of electronic quadrupoles in α-Ce is triple-**q** antiferroquadrupolar, as was suggested in Ref. [14]. We relate our findings to the current understanding of the $\gamma \to \alpha$ phase transition and also report on nuclear quadrupole interactions in other high-pressure phases of cerium: α'' ($C2/m$ space symmetry) and α' (α-U structure).

1. INTRODUCTION

Metallic cerium has a rich phase diagram with seven allotropic forms (α, β, γ, δ, α', α'', ϵ); its most puzzling issue is the isostructural $\gamma \to \alpha$ phase transition occurring at the pressure 0.7 GPa at room temperature and accompanied by near a 16 % volume collapse [1]. The transition was first observed in [2]. The face-centered cubic (fcc) character of both phases was established by pressure [3] and temperature [4] X-ray diffraction experiments in 1949 and 1950. The physical properties of the two phases are different. In the γ phase, the magnetic susceptibility $\chi(T)$ follows the Curie–Weiss law, but in the α phase, the overall temperature dependence of χ is very weak and paramagnetic. At a first glance, the $\gamma \to \alpha$ change contradicts the Landau theory of phase transitions [5], according to which a phase transition is usually accompanied by a change in symmetry, which is caused by an effective attractive interaction of the density–density type. This philosophy fails at the apparently isostructural phase transition in cerium.

The $\gamma \to \alpha$ change is probably a record-holder for the number of various models and theories attempted to explain it. In the first interpretation (a "promotional" model), the localized $4f$ electrons were thought to become a part of the $(6s5d)$ conduction band in α-Ce. According to the model, the γ and α phases should differ in the number of $4f$ electrons. The conclusion was checked by positron annihilation [6] and Compton scattering experiments [7]. Both mea-

*E-mail: tsvyash@hppi.troitsk.ru
**E-mail: alex_benik@yahoo.com

surements reported the same number of $4f$ electrons, thereby ruling out the promotional model.

In 1974, based on a thermodynamic analysis, Johansson proposed describing the $\gamma \to \alpha$ phase change as a Mott-like transition for the $4f$ electron subsystem [8]. The model implies approximately the same number of $4f$ electrons in both phases. In α-Ce, the $4f$ states participate in metallic bond formation, and different degrees of localization were considered in γ-Ce. Two fcc phases of cerium were attributed to the two local free-energy minima that develop for the same crystal structure ($Fm\bar{3}m$).

The concept of a Mott-like transition competes with the Kondo volume collapse theory [9, 10]. In the Kondo model, the $4f$ electrons remain localized under the $\gamma \to \alpha$ phase change. Further, the hybridization of the $4f$ orbitals with the conduction band leads to a singlet nonmagnetic state separated from the excited magnetic states by the Kondo energy $k_B T_K$. To describe the volume contraction under the $\gamma \to \alpha$ phase transition, theoretical models use the volume dependence of the Kondo temperature. Such a volume collapse leads to a phase instability without symmetry change and is interpreted as an isostructural transition.

These two concepts — the Kondo volume collapse [9, 10] and Mott-like transition for $4f$ electrons [8] — are permanently developing and becoming more and more sophisticated (see the references in [11] for recent development). Despite much efforts, there is still no consensus on the issue of the $\gamma \to \alpha$ phase transition in the scientific community [12]. It is also noteworthy that both these concepts took the isostructural nature of the $\gamma \to \alpha$ phase change as a well-established fact.

However, two theoretical works questioned the experimental conclusion [13, 14]. Eliashberg and Capellmann suggested that α-Ce should have a distorted fcc structure [13], which was in disagreement with the previous X-ray diffraction experiments. Recent high-quality X-ray diffraction experiments have found no distortions of the fcc structure [11]. At the same time, in a series of papers, Nikolaev and Michel developed a theory of hidden quadrupolar ordering in cerium [14–16] under the $\gamma \to \alpha$ phase change. The theory does not contradict X-ray diffraction data, but its main conclusion (symmetry lowering) requires experimental verification. In this paper, we report our results on probing the hidden quadupolar order in α-Ce (and other high-pressure cerium phases) with the technique of time differential perturbed angular correlation. We have found a hidden quadupolar order in α-Ce and for the first time have shown that the $\gamma \to \alpha$ phase transition in Ce is not isostructural.

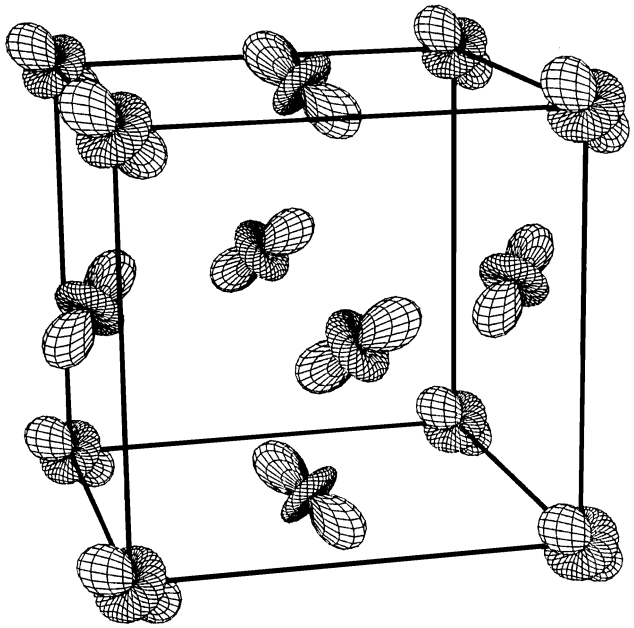

Fig. 1. Triple-**q** antiferroquadrupolar ($Pa\bar{3}$) structure of α-Ce proposed in [14]. Quadrupoles represent the $l = 2$ valence electron ($4f + 5d6s^2$) charge density distribution

2. QUADRUPOLAR ORDERING AND TRIGONAL SITE SYMMETRY IN THE α PHASE

According to the theory of quadrupolar ordering, the $\gamma \to \alpha$ transformation is not isostructural. Nevertheless, the electronic order parameter was overlooked because of a very particular symmetry change, as is shown in Fig. 1. The transition is of the first order and is driven by the minimization of the electron repulsion between the neighboring cerium sites. In the first formulation, only the repulsion between localized f-electrons was taken into account [14]. Later, a coupling with the conduction electrons was also included [15, 16]. The active electronic mode belongs to the X point of the Brillouin zone of the fcc lattice and involves its three arms, $\mathbf{q}_X^x$, $\mathbf{q}_X^y$, and $\mathbf{q}_X^z$. Here, the wave vectors are respectively given by $2\pi/a(1,0,0)$, $2\pi/a(0,1,0)$, and $2\pi/a(0,0,1)$ (a is the cubic lattice constant). To determine a possible symmetry lowering, the condensation schemes [17, 18] must be analyzed at the X point of the Brillouin zone and the scheme leading to the minimum of the free energy must be chosen. For cerium, the $Fm\bar{3}m \to Pa\bar{3}$ condensation scheme was suggested [14–16]. It involves three quadrupole density components of the T_{2g} symmetry, which alternate sign along x, y, and z axes, and that is why the or-

dered phase is termed the triple-**q** antiferroquadrupole (3-**q**-AFQ) structure.

In real space, the 3-**q**-AFQ ordering of the $Pa\bar{3}$ symmetry is characterized by four different sublattices of the simple cubic structure. We label the sublattices that contain the sites (0,0,0), $(a/2)(0,1,1)$, $(a/2)(1,0,1)$, and $(a/2)(1,1,0)$ by $\{\mathbf{n}_p\}$, $p = 1, 2, 3, 4$, respectively. The most significant feature of the ordered phase is the existence of only one three-fold C_3 symmetry axis at each cerium site, which is also a cube diagonal. The full site symmetry in this case is $S_6 = C_3 \times i$ (i is an inversion). The only quadrupole function compatible with the symmetry lowering is $Y_{\ell=2}^{m=0}(\Omega')$ in the coordinate system where the z' axis coincides with one of the three-fold axes (cube diagonals $[\rho_1, \rho_2, \rho_3]$): [111], $[\bar{1}, \bar{1}, 1]$, $[1, \bar{1}, \bar{1}]$, and $[\bar{1}, 1, \bar{1}]$. Consequently, there are four such functions, which are given by

$$\mathcal{S}_p = \frac{1}{\sqrt{3}} \left[\rho_1(p) Y_2^{1s} + \rho_2(p) Y_2^{1c} + \rho_3(p) Y_2^{2s} \right], \qquad (1)$$

where Y_2^{1s}, Y_2^{1c}, and Y_2^{2s} (proportional to the Cartesian components yz, zx, and xy) are real spherical harmonics [19], and the index $p = 1$–4 labels the sublattices. Thus, the quadrupole order is due to the local $Y_{\ell=2}^{m=0}$ charge density component of four valence electrons of cerium ($4f + 5d6s^2$) (see Fig. 1). This electron charge density component is considerably smaller than the spherically symmetric ($\ell = 0$) component built up from the 58 cerium electrons.

The space group symmetry lowering

$$Fm\bar{3}m(\gamma\text{-Ce}) \to Pa\bar{3}(\alpha\text{-Ce})$$

requires a uniform lattice contraction, and hence the fcc structure of the atomic center-of-mass points (cerium nuclei) is fully conserved [14, 16]. Thus, the quadrupole model not only agrees with previous experimental results and in particular with X-ray scattering data, but also reconciles the $\gamma \to \alpha$ transformation with the well-established Landau theory of phase transitions. The significance of this fact should not be underestimated. In particular, it implies that apart from the specific symmetry change, the $\gamma \to \alpha$ phase transition is not much different from other cerium transformations: $\alpha \to \alpha''$(monoclinic $C2/m$ symmetry), $\alpha'' \to \alpha'$(orthorhombic α-U space symmetry), etc. [1, 20]. It is also clear that other theoretical models for the $\gamma \to \alpha$ phase transition treat it as an exclusive case, not immediately applicable to other phase transformations. Unlike these other approaches, the theory of quadrupole ordering [14, 16] appealed to the experimental refinement of the electronic structure of α-Ce.

The phase transition of the $Fm\bar{3}m \to Pa\bar{3}$ type is not uncommon in molecular crystals. It occurs in fullerite C_{60} [21], nitrogen crystal (α-N_2) [22], etc. The problem with α-Ce is that the proposed space symmetry does not alter the fcc structure of the cerium nuclei. Nevertheless, a hidden 3-**q**-AFQ symmetry change was found experimentally in NpO_2 [23]. The phase transition in NpO_2 first detected at $T_0 = 25.5$ K by specific heat measurements was for many years considered isostructural [24, 25] like the $\gamma \to \alpha$ transition in cerium. In 2002, resonant X-ray scattering experiments at the Np M_{IV} and M_V absorption edges found the $Fm\bar{3}m \to Pn\bar{3}m$ symmetry lowering [23, 25]. The $Pn\bar{3}m$ symmetry is another triple-**q** structure, which differs from $Pa\bar{3}$ in the way the threefold axes and electronic quadrupoles are distributed over the four sublattices [26]. Thus, the case of NpO_2 created a precedent that should shake the classical understanding of "isostructural" phase transitions, and of the $\gamma \to \alpha$ transformation in cerium in particular.

3. EXPERIMENT

Capturing the suggested 3-**q**-AFQ order in α-Ce [14–16] is a formidable task. As in the case of NpO_2 [23, 25], one can resort to synchrotron radiation scattering experiments. But there are two experimental problems that hinder such an investigation. First, in addition to the expected small scattering intensity from the quadrupole components of electron valence density, the nontrivial domain structure of $Pa\bar{3}$ must also be taken into account. Second, upon cooling, the transition to α-Ce is hampered by the formation of the parasitic β-Ce. Further, if a single crystal is used, the volume change ("collapse") leads to the appearance of numerous cracks, which virtually destroy the crystal.

In this study of cerium allotropes, we used the sensitive technique of time-differential perturbed angular correlations (TDPAC), in which the electric field gradient (EFG) is targeted at impurity probe nuclei. Through the electric quadrupole hyperfine interaction, the electric field gradient at a lattice site is directly experienced by a probe nucleus. Such nuclear quadrupole interactions (QI) in solids are used in many techniques (for example, nuclear quadrupole resonance and Mössbauer spectroscopy). TDPAC is a less known technique [27] that uses nuclear probes inserted in the investigated lattice. It is worth noting that the TDPAC measurements can be performed with very few impurity nuclei and, in contrast to the Mössbauer spectroscopy, it is not restricted to low temperatures. In the best

cases, the method yields an accuracy approaching that of nuclear quadupole resonance.

Below, we report our results on the pressure dependence of the EFG and the quadrupole interaction frequency (QF) ν_Q proportional to it, measured at ^{111}Cd nuclei introduced in lattice sites of metallic cerium. Experiments have been carried out at room temperature and covered four phases of elemental cerium: γ, α, α'', and α' [1, 20]. The operator of the quadrupole interaction of the nuclear charge distribution in an external EFG is given by [27, 28]

$$H = \frac{1}{6}\sum_{i,j=1}^{3} Q_{ij}V_{ij}, \tag{2}$$

where Q_{ij} is the nuclear quadrupole moment operator defined by the corresponding integrals over the nuclear charge density, and $V_{ij} = \partial^2 V/\partial i \partial j$ $(i,j = x,y,z)$ is the EFG tensor at the ^{111}Cd nucleus. Being a symmetric traceless second-rank tensor, V_{ij} can be diagonalized. As a result, it is customary to characterize EFG by the largest principal component V_{zz} and the asymmetry parameter $\eta = (V_{xx} - V_{yy})/V_{zz}$ $(|V_{xx}| \le |V_{yy}| \le |V_{zz}|,\ 0 \le \eta \le 1)$ [27, 28].

The measurements of the nuclear quadrupole interaction of ^{111}Cd in cerium were performed using the 171–245-keV γ-ray cascade in ^{111}Cd populated by the electron capture decay of the ^{111}In isotope with the 2.8 day half-life. The cascade proceeds via the 245-keV level with the half-life $T_{1/2} = 84$ ns, spin $I = 5/2$, and the nuclear quadrupole moment $Q = 0.83$ b. The ^{111}In activity was produced via the ^{109}Ag $(\alpha, 2n)$ ^{111}In reaction by irradiating a silver foil with a 32-MeV α-beam. After that, the nuclear ^{111}In/^{111}Cd probes were introduced in the cerium lattice by melting Ce powder (about 500 mg) with a small piece of irradiated silver foil (less than 0.1 mg) in a special chamber under the pressure 8 GPa [29]. The TDPAC measurements were performed on polycrystalline samples of cerium metal at room temperature using a four-detector spectrometer equipped with a small-size hydraulic four-arm press with a capacity up to 300 ton [30]. The high pressure up to 8 GPa was produced in a calibrated "toroid"-type device with NaCl as a pressure-transmitting medium [31]. Nonhydrostaticity of the transmitting medium was checked by measuring the ^{111}Cd-TDPAC spectra of silver (fcc) under high pressure and observed to be negligibly small (Fig. 2).

The angular time correlation is characterized by the second-order perturbation factor of the static electric QI for the nuclear spin $I = 5/2$, which describes its precession due to the hyperfine interaction [27]:

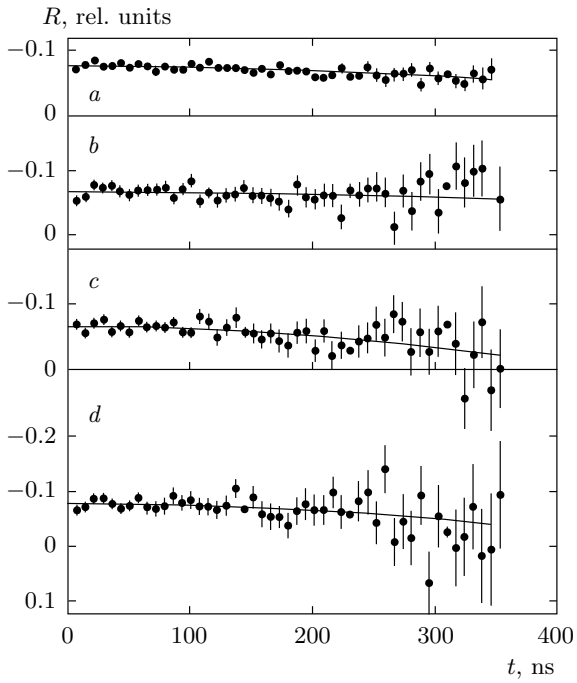

Fig. 2. Room-temperature TDPAC spectra of ^{111}Cd in silver ($Fm\bar{3}m$ symmetry) under pressure: a — ambient pressure, $\nu_Q = 0.2(1)$ MHz; b — $p = 3.15$ GPa, $\nu_Q = 0.2(2)$ MHz; c — $p = 5.55$ GPa, $\nu_Q = 0.3(2)$ MHz; d — $p = 8$ GPa, $\nu_Q = 0.3(2)$ MHz. The $R(t)$ spectrum remains very narrow with a small $\nu_Q = 0.2$–0.3 MHz, $\eta = 0$ even upon applying a high pressure of 8 GPa

$$G_{22}(t;\nu_Q,\eta,\Lambda) = \\ = s_{20} + \sum_{n=1}^{3} s_{2n}\cos(\omega_n t)\exp(-\Lambda_n\omega_n t). \tag{3}$$

Here, t is the time delay, s_{2n} are the amplitude coefficients, and ω_n are the angular precession frequencies $(n = 1,2,3$ for $I = 5/2)$ related to the energy differences between hyperfine levels split by the QI. The frequencies are functions of the EFG V_{zz} or, alternatively, of the QF

$$\nu_Q = eQV_{zz}/h \tag{4}$$

and the asymmetry parameter η (h is the Planc constant). Λ is the half-width of the QF Lorentzian distribution accounting for oscillatory damping.

Recording the delayed coincidence spectra at angles $\pi/2$ and π between detectors, $N(\pi/2,t)$ and $N(\pi,t)$, we obtain the usual angular anisotropy

$$R(t) = 2\frac{N(\pi,t) - N(\pi/2,t)}{N(\pi,t) + 2N(\pi/2,t)}, \tag{5}$$

which is the TDPAC spectrum. The pressure evolution of the TDPAC spectrum of ^{111}Cd in Ce is given in Fig. 3. It can be shown [27] that

$$R(t) = -A_{22}Q_2G_{22}(t), \qquad (6)$$

where $G_{22}(t)$ is the perturbation factor, Eq. (3), $Q_2 \approx \approx 0.80$ is the solid-angle correction, and $A_{22} = -0.17$ is the unperturbed angular correlation coefficient for the γ–γ cascade of ^{111}Cd. The EFG parameters are determined from the least-square fitting of the TDPAC spectra in accordance with Eq. (3).

4. RESULTS

The extensive TDPAC data are presently available for the ^{111}Cd impurity, for which the EFG as a function of temperature and pressure has been determined in several rare-earth (RE) metals [32, 33]. We note that the majority of RE metals crystallize in hexagonal structures, implying a nonzero EFG at the RE nuclei. In particular, the double hexagonal close-packed (dhcp) β phase of cerium has been thoroughly investigated in [34].

In the cubic symmetry, the first nontrivial electron charge density contribution at each site is described by the cubic harmonic K_4 (i. e., the multipole index $\ell = 4$), thus leaving no room for an EFG tensor: $V_{ij} = 0$. (With a very high accuracy, $V_{ij} = 0$ in the fcc lattice of silver, see Fig. 2.) Therefore, one should find $\nu_Q \approx 0$ and $V_{ij} \approx 0$ if both γ- and α-Ce are assumed to be isostructural. Instead, from the ^{111}Cd TDPAC spectra $R(t)$ of cubic phases (Fig. 3), we find that the conclusion holds only for γ-Ce, while in α-Ce, $\nu_Q \neq 0$ and $V_{ij} \neq 0$, signaling the appearance of a hidden quadrupole charge density component at the probe ^{111}Cd nuclei. We first describe the TDPAC spectrum of γ-Ce, Fig. 3*a*. A slight decrease of $R(t)$ with time can be ascribed to a broad distribution of QF centred at $\nu_Q = 3.0(5)$ MHz. Such a distribution is found in all cubic metals and is attributed to lattice defects and other impurities. We note that our TDPAC spectrum of γ-Ce is very close to the one observed in [34] (the upper panel on Fig. 1 in that paper) with the same value of ν_Q.

From the structural data, we know that the TDPAC spectra at pressures 1.8, 3.1, 3.9, and 4.4 GPa should be identified as belonging to the α-phase (Figs. 3*b*–*e*). They are consistent, and we obtain $\nu_Q = 11(1)$ MHz ($V_{zz} = 0.54(4) \cdot 10^{21}$ V·m^{-2}) and a uniaxial local site symmetry ($\eta = 0$) from fitting. The values of ν_Q and V_{zz} are close to the TDPAC parameters for β-Ce ($\nu_Q = 12.5(7)$ MHz, $V_{zz} = 0.61(4) \cdot 10^{21}$ V·m^{-2} [34]), and other noncubic phases of cerium (see Figs. 3 and

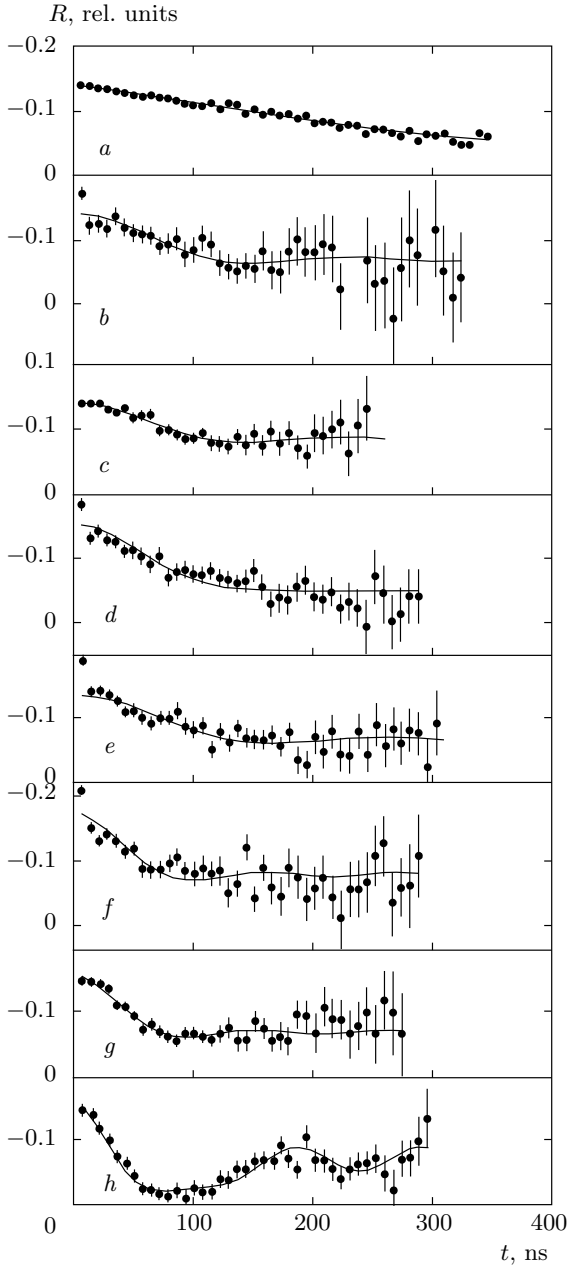

Fig. 3. Room-temperature TDPAC spectra of ^{111}Cd in cerium under pressure: *a* — at normal pressure, γ-Ce, fcc [$Fm\bar{3}m$] structure, no quadrupole order with $\nu_Q = 3.0(5)$ MHz and $\eta = 0$; *b*,*c*,*d* and *e* — α-Ce, 3-**q**-AFQ structure with $\nu_Q = 11(1)$, 10.9(6), 10.9(9), and 9.8(9) MHz and $\eta = 0$ at 1.8, 3.1, 3.9, and 4.4 GPa, respectively; *f* and *g* — α''-Ce [$C2/m$] with $\nu_Q = 15(1)$, 15.8(6) MHz and $\eta = 0$ at 5.3 and 6.2 GPa; *h* — α'-Ce [α-U structure] with $\nu_Q = 21.6(5)$ MHz and $\eta = 0.52(5)$ at 7.8 GPa

Table. The EFG V_{zz}, the asymmetry parameter η, and the QF frequency ν_Q for cerium under pressure p

p, GPa	ν_Q, MHz	η	V_{zz}, 10^{21} V·m^{-2}
0	3.0(5)	0	0.15(3)
1.8	11(1)	0	0.55(5)
3.1	10.9(6)	0	0.54(3)
3.9	10.9(9)	0	0.54(4)
4.4	9.8(9)	0	0.49(4)
5.3	15(1)	0	0.75(5)
6.2	15.8(6)	0	0.79(3)
7.8	21.6(5)	0.52(5)	1.08(3)

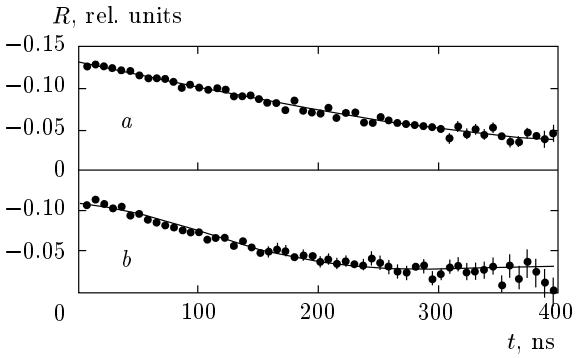

Fig. 4. TDPAC spectra of ^{111}Cd in γ-Ce ($Fm\bar{3}m$) at $T = 300$ K (a, $\nu_Q = 2.5(6)$ MHz) and in a sample (α-Ce?) quenched to $T = 77$ K (b, $\nu_Q = 5.5(3)$ MHz). At $T = 77$ K the spectrum has an increased value of $\nu_Q = 5.5$ MHz, $\eta = 0$, see text for details

5 and Table). The observed values of QF and EFG for α-Ce unambiguously rule out the cubic symmetry and indicate a hidden quadrupolar order in this phase. This experimental finding can be rationalized only by assuming a 3-**q**-AFQ order in α-Ce (see Fig. 1). The only theory predicting such a symmetry change for cerium was developed in [14, 16].

The α-phase can also be reached by cooling below $T = 96$ K. Therefore, it is instructive to measure the TDPAC spectrum $R(t)$ of α-Ce at low temperatures. However, this path is hampered by the appearance of the intermediate β phase, which seriously contaminates further investigations. It is known that the amount of β-Ce can be increased by thermal cycling a sample of cerium several times between room temperature and some lower temperature. This procedure was followed in [34], but the authors were able to obtain only 43 % of β-Ce, while the remaining fraction belonged to γ-Ce. This obstacle is rather disappointing. The authors of [35] preferred to alloy a sample of cerium with 7 at. % Sc to avoid the formation of parasitic β-Ce. Although the Sc/Th alloying solves the problem, the sample becomes contaminated as a result. In this study, we followed a naive way to avoid β-Ce and cooled our samples rapidly (by quenching) to 77 K to achieve the α phase. Then the measurements of $R(t)$ were being collected for 12 h. The resulting TDPAC spectrum is shown in Fig. 4, lower panel. We again observe an increase in EFG (ν_Q changes from 2.5–3 MHz (γ-Ce) to 5.5 MHz (α-Ce?)), which supports our conclusion for a substantial EFG in α-Ce. However, we admit that unlike in our pressure study, the situation here is not clear and further investigations are needed to clarify this issue.

The ^{111}Cd TDPAC spectra at pressures 5 to 8 GPa are shown in Figs. 3*f–h*. The spectrum at 5.3 GPa has the QF value 15 MHz, which is 1.5 times larger than the QF value at 4.4 GPa. Apparently, such an increase in the QF without a change of the asymmetry parameter ($\eta = 0$) is induced by the modification of the Ce crystal structure from the simple cubic symmetry ($Pa\bar{3}$) to the monoclinic α'' phase. A partial "softening" of the EFG and ν_Q in α-Ce at 4.4 GPa (ν_Q changes from 10.9(9) to 9.8(9) MHz) is also an indication of the proximity to the phase boundary. According to the angle-dispersive powder diffraction technique, the space symmetry of α''-Ce is $C2/m$ [20]. It follows from Figs. 3 and 5 and Table that the monoclinic $C2/m$ structure is preserved up to 7.5 GPa. At the pressure 7.8 GPa, the ^{111}Cd TDPAC spectrum characteristics change again. Now, the QF is 21.6(5) MHz ($V_{zz} = 1.08(3) \cdot 10^{21}$ V·m^{-2}) and the asymmetry parameter $\eta = 0.52(5)$. To elaborate the phase symmetry, we first note that according to Ref. [20], a sample of cerium preliminary heated to 373 K at 12 GPa (to the mixture of both the $C2/m$ and α-U phases) transforms to the α-U structure at a pressure above 7.5 GPa. Because our samples have been produced by melting at 8 GPa, they are also expected to undergo the transition to the α-U phase. We therefore conclude that the cerium phase at 7.8 GPa should be the orthorhombic (α-U) structure. The assignment is corroborated by a large value of η, which is characteristic of the α-U symmetry. (For elemental uranium in the α-phase, $\eta = 1$ [36].)

Figure 5 and Table present the overall pressure dependence of the QF and EFG in Ce. At the phase transition boundaries, the QF and EFG change discontinuously, indicating the first-order character of the transitions. The discontinuous behavior of QF with changes in the crystal structure was previously observed for a number of rare earths [32, 33].

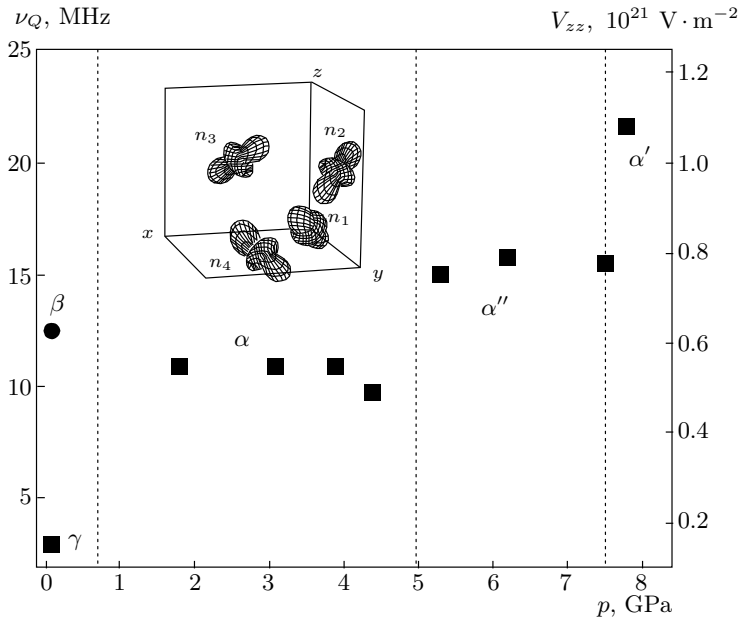

Fig. 5. Pressure dependence of the EFG V_{zz} and the QF frequency ν_Q for ^{111}Cd in cerium lattice: β is β-Ce from Ref. [34]; γ is γ-Ce with the fcc structure; α is α-Ce with a 3-**q**-AFQ structure shown in the insert, α' and α'' are α'-Ce (α-U) and α''-Ce ($C2/m$), respectively

5. CONCLUSIONS

Our TDPAC experiments (see Fig. 5 and Table) detect an appreciable EFG in α-Ce comparable with the EFG for noncubic phases (β, α''), which border α-Ce in the pressure–temperature phase diagram. This finding rules out the cubic symmetry in α-Ce and evidences in support of a 3-**q**-AFQ order suggested in [14], such that the local site symmetry is trigonal (C_3) with a quadrupolar electron charge density component $Y_{\ell=2}^{m=0}$ oriented along one of the main cube diagonals (see Fig. 1). For the first time, our experiments clearly indicate that the $\gamma \to \alpha$ phase transition is not isostructural, but they cannot determine the exact space symmetry group for α-Ce. Possible candidates are $Pa\bar{3}$ proposed in [14] and $Pn\bar{3}m$ found for NpO_2 in [23]. $Pa\bar{3}$ minimizes the electron–electron repulsion on neighboring sites, and $Pn\bar{3}m$ can win as a result of the f-electron participation in metal bond formation.

Upon quenching a sample of cerium to 77 K at normal pressure (where α-Ce is stable), we observe an increase in the EFG and ν_Q, consistent with our pressure measurements in α-Ce, although the increase is smaller than expected. We attribute the increase to the partial appearance of α-Ce, while an arrested fraction of γ-Ce and possibly of β-Ce contaminate the experiment.

In the pressure range 5–8 GPa (room temperature), the TDPAC spectrum follows other phase transitions in cerium: $\alpha \to \alpha''$ ($C2/m$) and $\alpha'' \to \alpha'$ (α-U structure). This direct correspondence demonstrates that the TDPAC method is a very sensitive tool for phase transformations.

Our main conclusion (that the $\gamma - \alpha$ phase transition in Ce is not isostructural) raises questions about other "isostructural" phase transitions. For example, $YbInCu_4$ exhibits a 0.5 % volume expansion without apparent change of symmetry upon cooling below $T = 42$ K [37]. We note that Yb in $YbInCu_4$ is the f-hole analog of Ce.

Finally, we remark on the disappearance of magnetic moments in α-Ce. Although the Kondo and Mott-like scenario cannot be excluded from further consideration, it is understood that the hidden symmetry change gives the problem a new dimension. In fact, the demagnetization of α-Ce can be rationalized in a simpler model [38]. We consider an instantaneous electron configuration of four coupled valence ($4f + 5d6s^2$) electrons at a cerium site. If the ground state of the system in γ-Ce is the magnetic triplet T_1 [T_2] (the maximum degeneracy in the cubic site symmetry group O_h) with magnetic moments $M_z = 0, \pm M$, then the trigonal crystal symmetry in α-Ce splits it into a magnetic doublet E (the maximum degeneracy in the trigonal site symmetry C_3) with $M_z = \pm M'$ and a nonmagnetic singlet A_1 [A_2]. If the A_1 [A_2] nonmagnetic state becomes the lowest, then the magnetic susceptibility χ at the

transition changes from Curie–Weiss-like behavior to a temperature-independent one [38].

This work is supported by the Program of the Presidium of RAS "Physics of Strongly Compressed Matter". We are grateful to S. M. Stishov, K. H. Michel, B. Verberck, A. N. Grum-Grzhimailo, and V. B. Brudanin for support of this work and discussion of the results.

REFERENCES

1. D. C. Koskenmaki and K. A. Gschneidner, Jr., in *Handbook on the Physics and Chemistry of Rare Earths*, ed. by K. A. Gschneidner, Jr. and L. Eyring North-Holland, Amsterdam (1978), Ch. 4, p. 337.
2. P. W. Bridgman, Proc. Amer. Acad. Arts Sci. **76**, 55 (1948).
3. A. W. Lawson abd T.-Y. Tang, Phys. Rev. **76**, 301 (1949).
4. A. F. Schuch and J. H. Sturdivant, J. Chem. Phys. **18**, 145 (1950).
5. L. D. Landau and E. M. Lifshitz, *Statistical Physics*, Nauka, Moscow (1995).
6. D. R. Gustafson, J. D. McNutt, and L. O. Roelling, Phys. Rev. B **183**, 435 (1969); R. F. Gempel, D. R. Gustafson, and J. D. Willenberg, Phys. Rev. B **5**, 2082 (1972).
7. U. Kornstädt, R. Lässer, and B. Lengeler, Phys. Rev. B **21**, 1898 (1980).
8. B. Johansson, Phil. Mag. **30**, 469 (1974).
9. J. W. Allen and R. M. Martin, Phys. Rev. Lett. **49**, 1106 (1982).
10. M. Lavagna, C. Lacroix, and M. Cyrot, Phys. Lett. A **90**, 210 (1982).
11. M. J. Lipp, D. Jackson, H. Cynn et al., Phys. Rev. Lett. **101**, 165703 (2008).
12. B. Johansson, A. V. Ruban, and I. A. Abrikosov, Phys. Rev. Lett. **102**, 189601 (2009).
13. G. Eliashberg and H. Capellmann, Pis'ma v Zh. Eksp. Teor. Fiz. **67**, 111 (1998).
14. A. V. Nikolaev and K. H. Michel, Eur. Phys. J. B **9**, 619 (1999).
15. A. V. Nikolaev and K. H. Michel, Eur. Phys. J. B **17**, 15 (2000).
16. A. V. Nikolaev and K. H. Michel, Phys. Rev. B **66**, 054103 (2002).
17. H. T. Stokes and D. M. Hatch, *Isotropy Subgroups of the 230 Crystallographic Space Groups*, World Scientific, Singapore (1988).
18. O. V. Kovalev, *Irreducible Representations of the Space Groups*, Gordon and Breach, New York (1965).
19. C. J. Bradley and A. P. Cracknell, *The Mathematical Theory of Symmetry in Solids*, Clarendon Press, Oxford (1972).
20. M. I. McMahon and R. J. Nelmes, Phys. Rev. Lett. **78**, 3884 (1997).
21. W. I. F. David, R. M. Ibberson, T. J. S. Dennis et al., Europhys. Lett. **18**, 219 (1992); P. A. Heiney, G. B. M. Vaughan, J. E. Fischer et al., Phys. Rev. B **45**, 4544 (1992).
22. T. A. Scott, Phys. Rep. **27**, 89 (1976).
23. J. A. Paixão, C. Detlefs, M. J. Longfield et al., Phys. Rev. Lett. **89**, 187202 (2002).
24. D. Malterre, M. Grioni, and Y. Baer, Adv. Phys. **45**, 299 (1996).
25. P. Santini, S. Carretta, G. Amoretti et al., Rev. Mod. Phys. **81**, 807 (2009).
26. A. V. Nikolaev and K. H. Michel, Phys. Rev. B **68**, 054112 (2003).
27. R. M. Steffen and H. Frauenfelder, in *Perturbed Angular Correlations*, ed. by E. Karlsson, E. Matthias, and K. Siegbahn, North-Holland, Amsterdam (1964).
28. E. N. Kaufmann and R. J. Vianden, Rev. Mod. Phys. **51**, 161 (1979).
29. A. V. Tsvyashenko, L. N. Fomicheva, A. A. Sorokin et al., Phys. Rev. B **65**, 174513 (2002).
30. V. B. Brudanin, D. V. Flossofov, O. I. Kochetov et al., Nucl. Instr. Meth. Phys. Res. A **547**, 389 (2005).
31. A. V. Tsvyashenko, L. N. Fomicheva, V. B. Brudanin et al., Phys. Rev. B **76**, 045112 (2007).
32. M. Forker, Hyperfine Interact. **24/26**, 907 (1985).
33. R. J. Vianden, Hyperfine Interact. **15/16**, 189 (1987).
34. M. Forker, L. Freise, and D. Simon, J. Phys. F **18**, 823 (1988).
35. A. P. Murani, Z. A. Bowden, A. D. Taylor et al., Phys. Rev. B **48**, 13981 (1993).
36. U. Hütten, R. Vianden, and E. N. Kaufmann, Hyperfine Interact. **34**, 213 (1987).
37. J. L. Sarrao, Physica B **259–261**, 128 (1999).
38. A. V. Nikolaev and K. H. Michel, Zh. Eksp. Teor. Fiz. **136**, 338 (2009).